CHEMISTRY OF MATERIALS

Article

pubs.acs.org/cm

Atomic Layer Deposition of Osmium

Jani Hämäläinen,*[,†] Timo Sajavaara,[‡] Esa Puukilainen,[†] Mikko Ritala,[†] and Markku Leskelä[†]

[†]Laboratory of Inorganic Chemistry, Department of Chemistry, University of Helsinki, P.O. Box 55, FI-00014 Helsinki, Finland

[‡]Accelerator Laboratory, Department of Physics, University of Jyväskylä, P.O. Box 35, FI-40014 Jyväskylä, Finland

ABSTRACT: Growth of osmium thin films and nanoparticles by atomic layer deposition is described. The Os thin films were successfully grown between 325 and 375 °C using osmocene and molecular oxygen as precursors. The films consisted of only Os metal as osmium oxides were not detected in X-ray diffraction measurements. Also the impurity contents of oxygen, carbon, and hydrogen were less than 1 at % each at all deposition temperatures. The long nucleation delay of the Os process facilitates either Os nanoparticle or thin film deposition. However, after the nucleation delay of about 350 cycles the film growth proceeded linearly with increasing number of deposition cycles. Also conformal growth of Os thin films on three-dimensional (3-D) structures was confirmed.

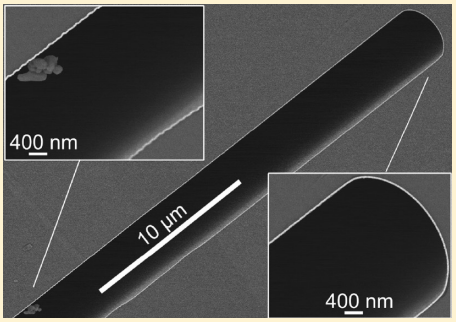

KEYWORDS: *atomic layer deposition, ALD, osmium, Os, noble metal, thin film, nanoparticle*

INTRODUCTION

Osmium is an interesting material among the noble metals. It competes with iridium for the title of the densest known natural element.[1] Os has a very low compressibility, that is, it has a high bulk modulus, which is comparable even to that of diamond;[2] however, Os is softer than diamond.[3] In a fine powdery or spongy form Os can oxidize easily in contact with air even at ambient conditions.[1] One of the oxides, OsO_4, is a dangerous and toxic compound with a very low boiling point.[1] At the same time Os has the highest melting point among noble metals when rhenium is not taken into account.[1] As a result of many properties of Os and its oxides, Os metal is a demanding material to manufacture and work with.

The number of Os thin film processes is quite limited; however, films, nanoparticles, and Os doped films have been grown with various methods, such as chemical vapor deposition (CVD),[4−11] sol−gel technique,[12−15] vacuum pyrolysis,[16] electrodeposition,[17] and physical vapor deposition (PVD).[18] Also thermal and plasma CVD have been used to deposit OsO_2 films.[8,19]

As for the applications of the Os, it is interesting to note that osmium appears in patent literature relating to catalysis, fuel cells, sensors, and electronic devices.[20] Compared to the other noble metals, however, the patent literature on Os is quite small in numbers.[21] Os metal is usually alloyed with other noble metals for use in electrical contacts, instrument pivots, fountain pen tips, and phonograph needles.[1] The use of Os thin films and nanoparticles in some nanoscale applications is briefly described here.

Os thin films have been suggested as adhesion layers and diffusion barriers for damascene metallizations.[18] Os doped SnO_2 sensors have been examined for methane sensing,[12,14] where the Os doping enhances the sensitivity and lowers the operating temperatures.[12,13] Os and Os−Pd nanoparticles on carbon nanotubes have been studied for catalysis.[16] It was shown that the Os−Pd nanoparticle catalysts utilize carbon nanotubes as a carbon source to produce new carbon nanotubes at elevated temperatures.[16] These catalysts were later used for one-step CVD preparation of metal nanoparticle coated carbon nanotubes from propylene.[16] Os nanoparticles have also been demonstrated as anodes in direct borohydride fuel cells.[22] The authors state that Os is a kinetically superior and stable catalyst for borohydride electro-oxidation in comparison to PtRu and Pt.[22] In addition, three-dimensional (3-D) anode structures could be interesting to be used in the direct borohydride fuel cells.[22]

Atomic layer deposition (ALD)[23−26] is a modification of the CVD method and deposits conformal and uniform thin films with precise thickness control. Most noble metal ALD processes use molecular oxygen as another reactant. The noble metals activate O_2 by catalyzing its dissociation to adsorbed oxygen atoms, which in turn react with noble metal precursor ligands during the following precursor pulse.[27,28] The rest of the ligand species of the noble metal precursor are combusted on the surface during the oxygen pulse and adsorbed oxygen layer forms again.[27,28] This oxygen-based noble metal chemistry has been successful for ruthenium,[29] rhodium,[30] iridium,[31] and platinum[32] metals while palladium[33,34] has been grown from a fluorinated β-diketonate precursor using reductants such as glyoxylic acid, molecular H_2, and formalin. Silver and gold are very demanding to be deposited by ALD because of the lack of suitable precursors which would be thermally stable as well as reactive enough. However, plasma enhanced ALD has proven feasible to deposit Ag films with hydrogen plasma.[35,36] Besides gold, also osmium ALD processes have been lacking.

Received: June 23, 2011
Revised: September 21, 2011
Published: December 9, 2011

 © 2011 American Chemical Society dx.doi.org/10.1021/cm201795s | *Chem. Mater.* 2012, 24, 55−60

In this study we present the growth of Os metal thin films and nanoparticles for the first time using oxygen-based thermal ALD chemistry and thereby add Os to the list of materials that can be deposited using ALD with all of its beneficial features. The oxygen-based ALD noble metal processes can be readily mixed and fine-tuned in composition for deposition of binary noble metal nanoparticles and thin films.[37−39] This should be feasible also with ALD Os, which would be very interesting application wise.

EXPERIMENTAL SECTION

Osmium thin films and nanoparticles were grown in a hot-wall flow-type F-120 ALD reactor (ASM Microchemistry Ltd., Finland) operated under a nitrogen pressure of about 5−10 mbar. Nitrogen was produced with a Domnick Hunter G2100E nitrogen generator and used as both a carrier and a purging gas. Os was grown from osmocene ($OsCp_2$, 99.9%, Strem) and O_2 (99.9999%, Aga) on in situ grown Al_2O_3 films. About 10 nm thick Al_2O_3 films were deposited by ALD (100 cycles) using $AlCl_3$ (99%, Alfa Aesar) and deionized water on top of 5 × 5 cm^2 silicon (111) and soda lime glass substrates. The solid $OsCp_2$ and $AlCl_3$ precursors were sublimed from open boats held inside the reactor at 80 °C and pulsed with inert gas valving. Deionized water was held in an external vessel at room temperature (RT) and pulsed into the reactor through needle and solenoid valves. Flow rate of O_2 was set to 5 sccm by a needle valve and a mass flow meter during continuous flow, and O_2 was pulsed into the reactor with a solenoid valve. Thermogravimetric analysis (TGA) of $OsCp_2$ was done in a flowing nitrogen atmosphere (1 atm) with a heating rate of 10 °C/min by a Mettler Toledo Star system equipped with a TGA 850 thermobalance.

Crystallinity of the films was examined with a PANalytical X'Pert Pro X-ray diffractometer using CuK_α-radiation. X-ray diffraction (XRD) patterns were measured using θ−2θ and grazing incidence (GIXRD) modes. Film thicknesses were determined from X-ray reflectivity (XRR) patterns measured with a Bruker AXS D8 Advance diffractometer. Surface morphology of the films was examined by a Hitachi S-4800 field emission scanning electron microscope (FESEM). Some film thicknesses were also analyzed using a GMR electron probe thin film microanalysis program[40] and energy-dispersive X-ray spectroscopy (EDX) data from an Oxford INCA 350 microanalysis system connected to the FESEM. Film resistivities were calculated from sheet resistances measured with a four-point probe technique and from the film thicknesses obtained from the XRR patterns. Adhesion of the films was tested with the common Scotch tape test. Impurity contents of the films were determined with time-of-flight elastic recoil detection analysis (TOF-ERDA)[41] by a 1.7 MV Pelletron accelerator using a 10.215 MeV $^{35}Cl^{5+}$ ion beam and full Monte Carlo simulations.

For atomic force microscopy (AFM) studies a Multimode V equipped with Nanoscope V controller (Veeco Instruments) was used. Image processing and data analysis were performed with NanoScope software version 7.30. Samples were measured in tapping mode in air using phosphorus-doped silicon probe (RTESP) delivered by Veeco Instruments. Both tapping mode topography and phase images were measured. Several scans were performed from different parts of the samples to check the uniformity of the surface. Final images were measured from a scanning area of 2 × 2 μm^2 with a scanning frequency of 0.5 Hz and no image processing except flattening was made. Roughness values were calculated as root-mean-square values (R_q).

Caution! *It is emphasized that Os metal can easily form dangerous OsO_4 gas under oxidizing conditions and at elevated temperatures.* Both these conditions are met in this work as oxygen is used in the combustion type ALD process at temperatures over 300 °C. Therefore, care must be taken for deposition of Os films and handling of the films after deposition. This includes proper cooling of the ALD reactor before exposing the Os film to ambient atmosphere as the boiling point of OsO_4 is as low as 130 °C.[1] In addition, powdered or spongy Os metal may also slowly form OsO_4 at room temperature.[1]

RESULTS AND DISCUSSION

Evaporation and thermal stability of $OsCp_2$ was studied with TGA (Figure 1). The evaporation starts at around 110 °C and

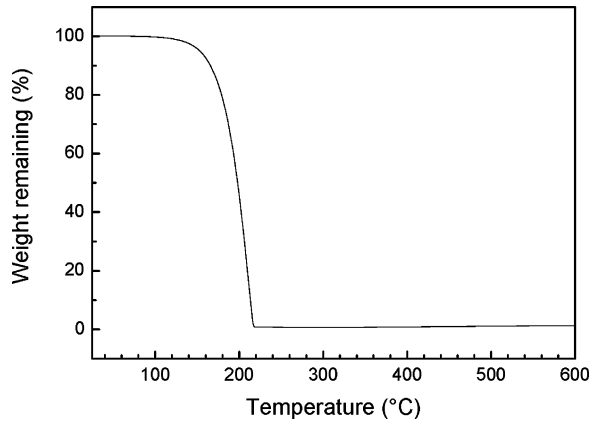

Figure 1. TGA curve measured for $OsCp_2$ under flowing N_2 atmosphere (1 atm).

reaches completion at 220 °C under flowing atmospheric pressure N_2. The residue at the end of the step is 1.3% of the initial weight of 5.5 mg. This indicates that $OsCp_2$ sublimes in one step without any substantial decomposition, which in turn means that $OsCp_2$ can be considered as a good precursor candidate for ALD. The normal atmospheric pressure TGA measurement can be used to estimate the appropriate source temperature to be used in a specific ALD reactor,[42] such as the F-120 ALD reactor used in this study. The source temperature was, however, optimized as low as possible (80 °C) to minimize the consumption of the expensive precursor.

Deposition of Os films was studied using $OsCp_2$ and O_2 as precursors. Relatively low flow rate of 5 sccm was chosen for O_2 to minimize the risk of formation of osmium oxides. OsO_4 in particular would be problematic because it is volatile and would therefore lead to etching of the film. First the deposition parameters, that is, the pulse lengths of $OsCp_2$ and O_2, were optimized at 350 °C (Figure 2). The film growth rate seems to slightly increase with increasing $OsCp_2$ pulse length; however, the $OsCp_2$ pulse lengths of 2 s and more result in a constant growth rate of about 0.3 Å/cycle (Figure 2a). Varying the O_2 pulse length between 1 and 4 s results also in a constant growth rate of about 0.3 Å/cycle (Figure 2b), which indicates that the relatively low O_2 flow rate of 5 sccm is well enough for complete combustion of the Cp ligands and that no etching occurs even when longer O_2 pulses are used. It should also be noted that the films remain fully reflective and mirror-like regardless of the length of the O_2 pulse. In some ALD Ru processes the films have been reported to become slightly milky in appearance with the high O_2 doses, which is related to the increased roughness of the films.[43] Besides considerable roughness, light scattering milky appearance may also indicate partial delamination of the film.[44] In addition, high O_2 flow rates, and hence high O_2 doses, have resulted in formation of RuO_2 instead of Ru metal under specific ALD conditions.[45]

The film thickness as a function of the number of the deposition cycles was examined after optimizing the pulse lengths for both $OsCp_2$ and O_2 precursors (Figure 3). The process shows substantial incubation delay as no film was observed after 300 deposition cycles. However the film thickness increases linearly with increasing deposition cycles between 500 and 1500 cycles.

dx.doi.org/10.1021/cm201795s | Chem. Mater. 2012, 24, 55−60

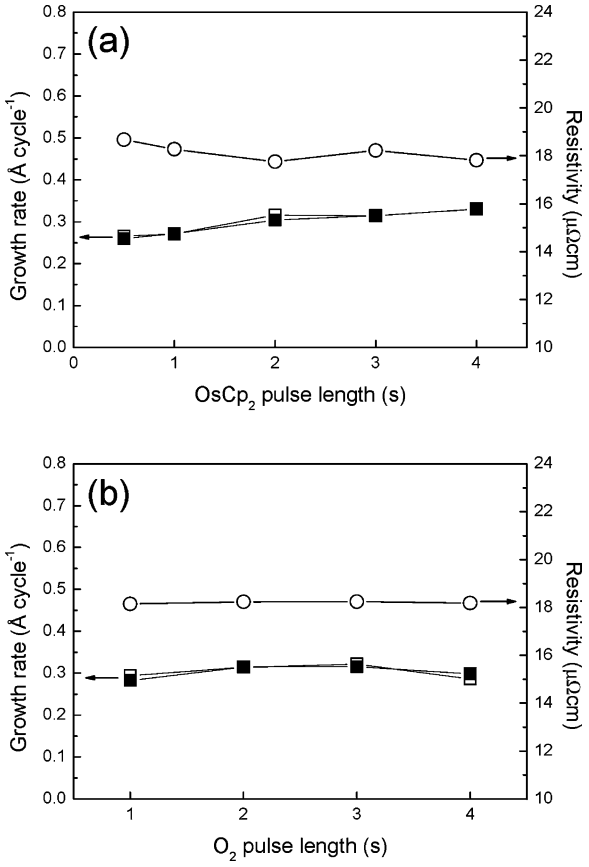

Figure 2. Growth rates and resistivities of the Os films grown on Al_2O_3 films at 350 °C as a function of (a) $OsCp_2$ and (b) O_2 pulse lengths. Both soda lime glass (open symbol) and Si (solid symbol) substrates were used. The pulse lengths for (a) O_2 and (b) $OsCp_2$ were 2 and 3 s, respectively. All the purges were 1 s each. The total number of $OsCp_2$–O_2 cycles was 1000.

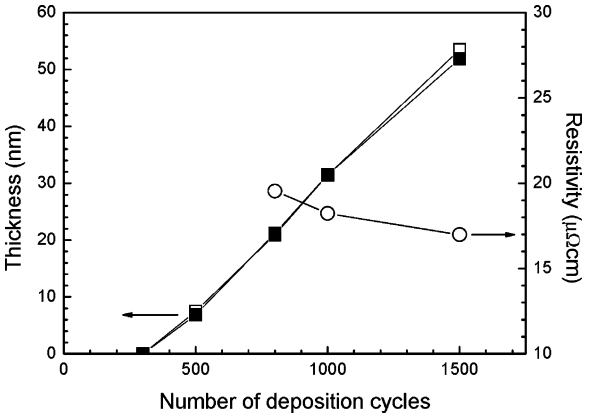

Figure 3. Thicknesses and resistivities of the Os films on Al_2O_3 films as a function of deposition cycles at 350 °C. $OsCp_2$ and O_2 pulses were 3 and 2 s, respectively, with 1 s purges. Open and solid symbols denote Os films on Al_2O_3 coated soda lime glasses and Si substrates, respectively.

The slope of the thickness curve suggests linear film growth after roughly 350 deposition cycles. After the nucleation period the growth rate is about 0.45 Å/cycle, which is substantially larger than the 0.3 Å/cycle measured from the films grown by 1000 cycles (Figure 2). This is simply because the latter value does not take into the account the nucleation delay.

Os thin films were successfully deposited between 325 and 375 °C on Al_2O_3 film (Figure 4). The films grown at 300 °C

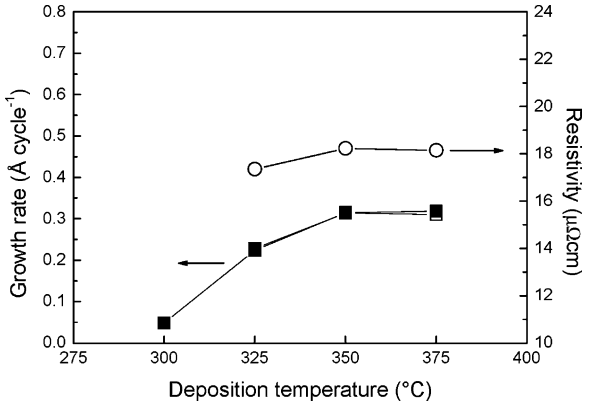

Figure 4. Growth rates and resistivities of the Os films on the Al_2O_3 surface as a function of deposition temperature. $OsCp_2$ and O_2 pulses were 3 and 2 s, respectively, with 1 s purges. 1000 cycles were applied in each deposition. Open and solid symbols denote Os films on Al_2O_3 coated soda lime glasses and Si substrates, respectively.

were very thin and nonuniform after 1000 cycles; therefore the low limit for this ALD process was considered to be 325 °C on the in situ grown Al_2O_3. The growth rates including the nucleation delays were roughly 0.2 Å/cycle at 325 °C and 0.3 Å/cycle between 350 and 375 °C (Figure 4). The increase of the growth rate with increasing deposition temperature is common to oxygen-based noble metal ALD processes and is contributed to some extent also by shorter nucleation delays at higher temperatures. In ALD of noble metals, Ru in particular, the use of other noble metals as starting surfaces has been shown to facilitate film growth at 50–75 °C lower temperatures than possible on an oxide surface.[46] Therefore, it is most likely that on the noble metal nucleation layer also the ALD Os process would deposit films at temperatures lower than 325 °C and with a shorter nucleation delay than on Al_2O_3.

The resistivities of the Os films grown on Al_2O_3 coated soda lime glasses are presented in Figures 2–4. The resistivities decreased from about 20 to 17 μΩ cm with increasing film thickness from about 20 to 50 nm (Figure 3). However, the resistivity of the Os film after 500 cycles could not be reliably measured from the Al_2O_3 coated substrates. The resistivities were independent of precursor pulse lengths (Figure 2). About 30 nm thick Os films had resistivities of about 18–19 μΩ cm with the studied $OsCp_2$ and O_2 pulse lengths. Similar resistivities were obtained between 325 and 375 °C (Figure 4); however, the film grown at the lowest temperature was a bit thinner. Os thin films grown by CVD from $OsCp_2$ and air or oxygen have been reported to have resistivities of 18 μΩ cm,[9] which are comparable to our results. The bulk resistivity (0 °C) of Os metal is 8.1 μΩ cm, which is slightly higher than that of Ru metal (7.1 μΩ cm).[1]

Film growth was studied also at 400 °C; however, most of the metallic film was etched away. This indicates that Os is quite reactive at higher temperatures, and possibly high oxygen doses could cause partial etching at lower temperatures as well. However, this was not observed with the O_2 flow rate (5 sccm) and O_2 pulse lengths (1–4 s) used in our study (Figure 2b). It should be emphasized that although etching was observed at 400 °C the $OsCp_2$ precursor did not show any signs of thermal decomposition at this temperature. In addition, about 20 to 30 nm thick films deposited between 325 and 375 °C (Figure 4) passed the tape test, which indicates that the adhesion of the Os films to Al_2O_3 is good.

dx.doi.org/10.1021/cm201795s | *Chem. Mater.* 2012, 24, 55–60

The crystallinity and composition of the grown films were examined using XRD measurements in both the $\theta-2\theta$ and GIXRD modes. The films deposited between 325 and 375 °C were hexagonal polycrystalline metallic Os (Figure 5). Only Os

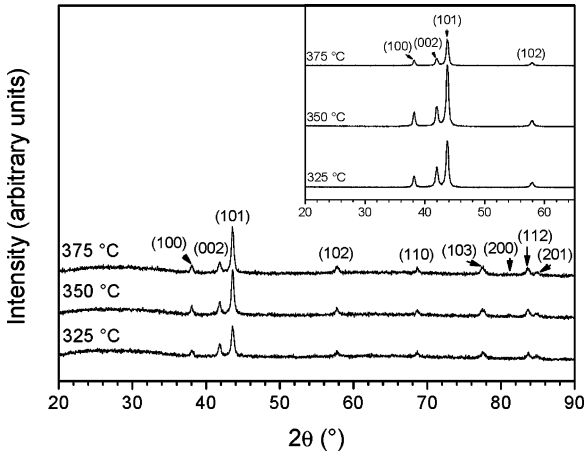

Figure 5. $\theta-2\theta$ XRD patterns of the Os films deposited between 325 and 375 °C. The substrate was soda lime glass with an Al_2O_3 nucleation layer. The inset shows GIXRD patterns of the Os films grown on Al_2O_3 coated Si. 1000 cycles were applied using 3 s $OsCp_2$ and 2 s O_2 pulses with 1 s purges.

with strong (101) reflection was observed from the measured $\theta-2\theta$ XRD and GIXRD patterns. It should be emphasized that no oxide phases such as OsO_2 could be seen in the films grown between 325 and 375 °C (Figure 5). The film purity was also verified by TOF-ERDA measurements (Table 1). The Os film

Table 1. Impurity Contents (TOF-ERDA) of the Os Films Deposited between 325 and 375 °C

dep. temp. (°C)	O (at %)	C (at %)	H (at %)
325	<1	0.5 ± 0.3	0.5 ± 0.4
350	<0.5	<0.2	<0.3
375	<0.5	0.5 ± 0.3	0.5 ± 0.4

grown at 350 °C contained only less than 0.5 at % oxygen, 0.2 at % carbon, and 0.3 at % hydrogen impurities. Overall, the films deposited between 325 and 375 °C were pure as the O, C, and H contents were each less than 1 at % at all deposition temperatures. In addition, some surface nitrogen was observed in all samples.

FESEM and AFM were used to study the morphology of the Os films. The films grown using the same number of cycles (1000) at 325, 350, and 375 °C show clearly that the deposition temperature has an effect on the grain sizes of the films (Figure 6). The thinnest film grown at the lowest temperature (325 °C) contains a substantial amount of large grains among smaller ones, whereas the film deposited at 375 °C is more uniform in grain size. It has been observed in the ALD Ru process using $RuCp_2$ and O_2 as precursors that the nucleation delay is shorter at higher deposition temperatures.[29] Similarly, it is reasonable to assume that in this ALD Os process the nucleation delay is the longest at the lowest deposition temperature. The long nucleation delay allows the grains to nucleate and start to grow at different times and thus some individual grains emerge earlier than the others. In the following cycles these grains are able to grow in size while new nuclei still appear. The grains grow, coalesce, and finally form a continuous film. As the film growth is retarded for the longest time at the lowest temperature (325 °C), the first formed grains have had more time to develop until a continuous film has been formed; therefore, the formation of large grains is more pronounced at the lowest temperature (Figure 6). Similarly, rms surface roughness decreases as a function of deposition temperature: 2.8 nm at 325 °C, 2.0 nm at 350 °C, and 1.5 nm at 375 °C, respectively (Figure 6).

The stepwise formation of a continuous Os film at 350 °C is seen in Figure 7. The thicknesses are based on the EDX data, which was converted to film thicknesses assuming uniform film and a density of 22 g/cm^3. These thicknesses vary slightly from the XRR thicknesses (Figure 4); however, the difference decreases with thicker films. After 300 cycles of the $OsCp_2-O_2$ process there are only some scattered separate grains of uneven size on the Al_2O_3 surface. The film after 500 cycles is not fully continuous and contains some voids; however, the 25 nm thick film after 800 cycles is continuous. The grain size increases with increasing film thickness while the overall size distribution of the grains is not so pronounced as in the thinner films (Figure 7). With this $OsCp_2-O_2$ ALD process it is possible to deposit continuous and conformal Os films on 3-D structures such as trenches shown in Figure 8. The FESEM specimen was made just by breaking the substrate after the deposition, which caused some defects seen in the low magnification image in Figure 8.

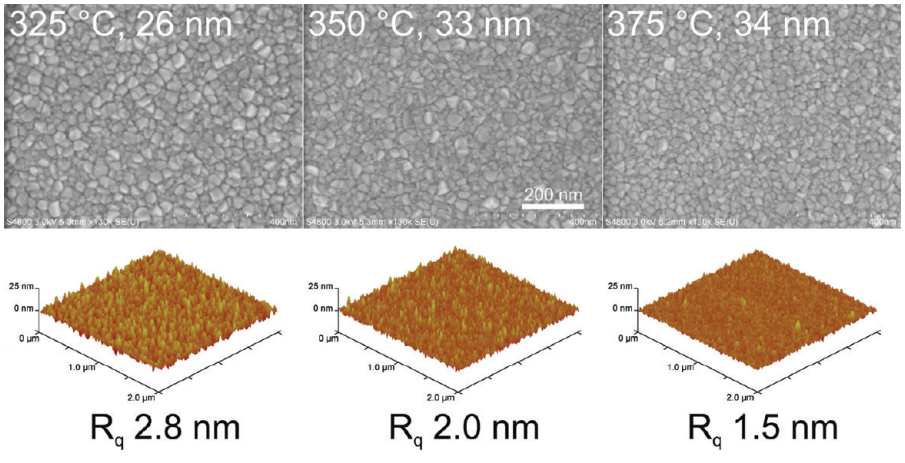

Figure 6. FESEM and AFM images of the Os films grown on the Al_2O_3 surface at various deposition temperatures. The deposition temperatures, film thicknesses obtained from EDX data, and surface roughnesses (R_q) are shown in the images.

dx.doi.org/10.1021/cm201795s | Chem. Mater. 2012, 24, 55–60

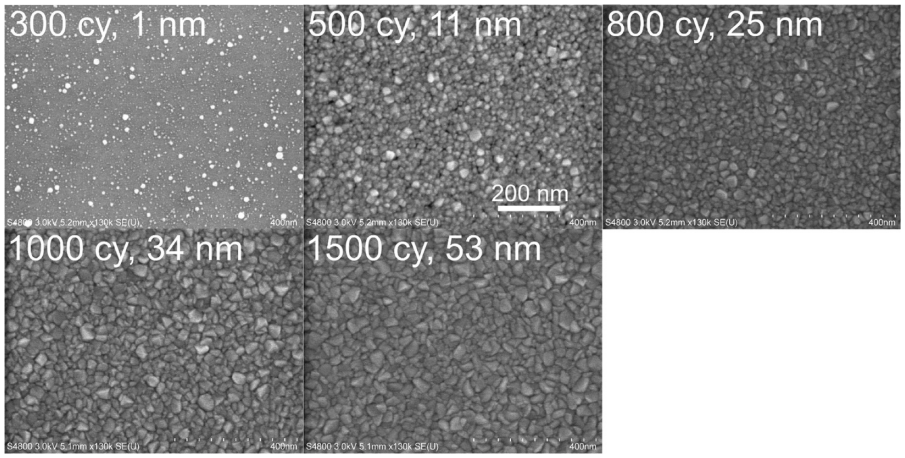

Figure 7. FESEM images of the Os films grown on the Al_2O_3 surface at various number of deposition cycles. The number of cycles applied and film thicknesses obtained from EDX data are shown in the images.

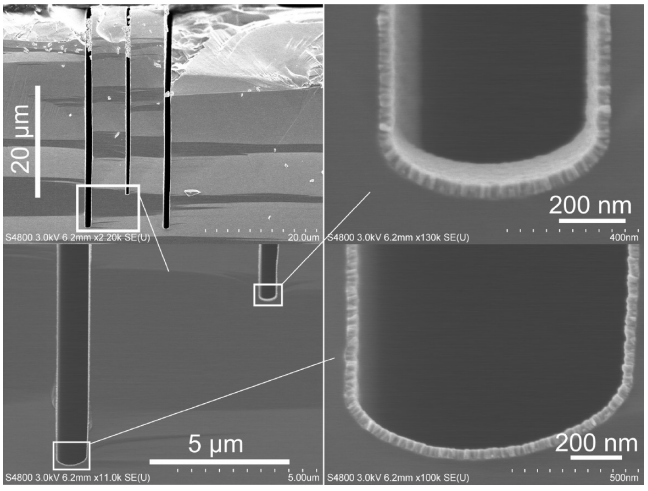

Figure 8. FESEM images of the Os film grown on in situ Al_2O_3 coated trench structure at 350 °C using 1000 deposition cycles.

In conclusion, Os films were successfully grown by ALD between 325 and 375 °C using $OsCp_2$ and O_2 as precursors. According to XRD and TOF-ERDA all the films consisted of only metallic Os. The films were also pure as C, O, and H impurity contents were less than 1 at % each. The surface roughnesses of about 30 nm thick films were 1.5−3 nm and smoother films were grown at higher temperatures. The saturation of the growth rate with respect of both precursors was verified at 350 °C. The ALD Os process has a substantial nucleation delay of about 350 cycles at 350 °C on the Al_2O_3 surface, which means that either Os nanoparticles or Os thin films can be easily deposited by simply adjusting the number of deposition cycles. It was shown also that by ALD Os films can be deposited on 3-D structures in a conformal manner.

AUTHOR INFORMATION

Corresponding Author

*E-mail: jani.hamalainen@helsinki.fi. Fax: +358 9 191 50198.

ACKNOWLEDGMENTS

Financial funding from ASM Microchemistry Ltd. is gratefully appreciated. Timo Hatanpää is thanked for assisting in the TGA measurement. Furthermore, the Finnish Centre of Excellence Programme 200620100 (Project No. 213503, Nuclear and Accelerator Physics Programme at JYFL) is gratefully acknowledged for TOF-ERDA.

REFERENCES

(1) *CRC Handbook of Chemistry and Physics*, 91st ed. (Internet Version 2011); Haynes, W. M., Ed.; CRC Press/Taylor and Francis: Boca Raton, FL, 2011.
(2) Cynn, H.; Klepeis, J. E.; Yoo, C.-S.; Young, D. A. *Phys. Rev. Lett.* **2002**, *88*, 135701.
(3) Sahu, B. R.; Kleinman, L. *Phys. Rev. B* **2005**, *72*, 113106.
(4) Akahori, H.; Handu, M.; Yoshida, H.; Kozuka, Y. *J. Electron. Microsc.* **2000**, *49*, 735.
(5) Boyd, E. P.; Ketchum, D. R.; Deng, H.; Shore, S. G. *Chem. Mater.* **1997**, *9*, 1154.
(6) Chi, Y.; Yu, H.-L.; Ching, W.-L.; Liu, C.-S.; Chen, Y.-L.; Chou, T.-Y.; Peng, S.-M.; Lee, G.-H. *J. Mater. Chem.* **2002**, *12*, 1363.
(7) Li, C.; Leong, W. K.; Loh, K. P. *Appl. Organomet. Chem.* **2009**, *23*, 196.
(8) Senzaki, Y.; Colombo, D.; Gladfelter, W. L.; McGormick, F. B. *Proc. Electrochem. Soc.* **1997**, *97−25*, 933.
(9) Smart, C. J.; Gulhati, A.; Reynolds, S. K. *Mater. Res. Soc. Symp. Proc.* **1995**, *363*, 207.
(10) Berry, A. D.; Brown, D. J.; Kaplan, R.; Cukauskas, E. J. *J. Vac. Sci. Technol. A* **1986**, *4*, 215.
(11) Yu, H.-L.; Chi, Y.; Liu, C.-S.; Peng, S.-M.; Lee, G.-H. *Chem. Vap. Deposition* **2001**, *7*, 245.
(12) Quaranta, F.; Rella, R.; Siciliano, P.; Capone, S.; Epifani, M.; Vasanelli, L.; Licciulli, A.; Zocco, A. *Sens. Actuators B* **1999**, *58*, 350.
(13) Siciliano, P. *Sens. Actuators B* **2000**, *70*, 153.
(14) Epifani, M.; Forleo, A.; Capone, S.; Quaranta, F.; Rella, R.; Siciliano, P.; Vasanelli, L. *IEEE Sens. J.* **2003**, *3*, 827.
(15) Forleo, A.; Capone, S.; Epifani, M.; Siciliano, P.; Rella, R. *Appl. Phys. Lett.* **2004**, *84*, 744.
(16) Yung, K.-F.; Wong, W.-T. *J. Cluster Sci.* **2006**, *18*, 51.
(17) Jones, T. *Met. Finish* **2002**, *100*, 84.
(18) Josell, D.; Witt, C.; Moffat, T. P. *Electrochem. Solid-State Lett.* **2006**, *9*, C41.
(19) Hayakawa, Y.; Fukuzaki, K.; Kohiki, S.; Shibata, Y.; Matsuo, T.; Wagatsuma, K.; Oku, M. *Thin Solid Films* **1999**, *347*, 56.
(20) Seymour, R. *Platinum Met. Rev.* **2006**, *50*, 27.
(21) Seymour, R. *Platinum Met. Rev.* **2008**, *52*, 231.
(22) Lam, V. W. S.; Gyenge, E. L. *J. Electrochem. Soc.* **2008**, *155*, B1155.
(23) Ritala, M.; Leskelä, M. In *Handbook of Thin Film Materials*; Nalwa, H. S.; Ed.; Academic Press: San Diego, CA, 2001; Vol. *1*, pp 103−159.
(24) Puurunen, R. L. *J. Appl. Phys.* **2005**, *97*, 121301.

(25) Ritala, M.; Niinistö, J. In *Chemical Vapor Deposition: Precursors, Processes and Applications*; Jones, A. C., Hitchman, M. L.; Eds.; The Royal Society of Chemistry: Cambridge, U.K., 2009; pp 158−206.
(26) George, S. M. *Chem. Rev.* **2010**, *110*, 111.
(27) Aaltonen, T.; Rahtu, A.; Ritala, M.; Leskelä, M. *Electrochem. Solid-State Lett.* **2003**, *6*, C130.
(28) Knapas, K.; Ritala, M. *Chem. Mater.* **2011**, *23*, 2766.
(29) Aaltonen, T.; Alén, P.; Ritala, M.; Leskelä, M. *Chem. Vap. Deposition* **2003**, *9*, 45.
(30) Aaltonen, T.; Ritala, M.; Leskelä, M. *Electrochem. Solid-State Lett.* **2005**, *8*, C99.
(31) Aaltonen, T.; Ritala, M.; Sammelselg, V.; Leskelä, M. *J. Electrochem. Soc.* **2004**, *151*, G489.
(32) Aaltonen, T.; Ritala, M.; Sajavaara, T.; Keinonen, J.; Leskelä, M. *Chem. Mater.* **2003**, *15*, 1924.
(33) Senkevich, J. J.; Tang, F.; Rogers, D.; Drotar, J. T.; Jezewski, C.; Lanford, W. A.; Wang, G.-C.; Lu, T.-M. *Chem. Vap. Deposition* **2003**, *9*, 258.
(34) Elam, J. W.; Zinovev, A.; Han, C. Y.; Wang, H. H.; Welp, U.; Hryn, J. N.; Pellin, M. J. *Thin Solid Films* **2006**, *515*, 1664.
(35) Niskanen, A.; Hatanpää, T.; Arstila, K.; Leskelä, M.; Ritala, M. *Chem. Vap. Deposition* **2007**, *13*, 408.
(36) Kariniemi, M.; Niinistö, J.; Hatanpää, T.; Kemell, M.; Sajavaara, T.; Ritala, M.; Leskelä, M. *Chem. Mater.* **2011**, *23*, 2901.
(37) Christensen, S. T.; Feng, H.; Libera, J. L.; Guo, N.; Miller, J. T.; Stair, P. C.; Elam, J. W. *Nano Lett.* **2010**, *10*, 3047.
(38) Jiang, X.; Gür, T. M.; Prinz, F. B.; Bent, S. F. *Chem. Mater.* **2010**, *22*, 3024.
(39) Comstock, D. J.; Christensen, S. T.; Elam, J. W.; Pellin, M. J.; Hersam, M. C. *Adv. Funct. Mater.* **2010**, *20*, 3099.
(40) Waldo, R. A. *Microbeam Anal.* **1988**, *23*, 310.
(41) Putkonen, M.; Sajavaara, T.; Niinistö, L.; Keinonen, J. *Anal. Bioanal. Chem.* **2005**, *382*, 1791.
(42) Niskanen, A.; Hatanpää, T.; Ritala, M.; Leskelä, M. *J. Therm. Anal. Calorim.* **2001**, *64*, 955.
(43) Aaltonen, T.; Ritala, M.; Arstila, K.; Keinonen, J.; Leskelä, M. *Chem. Vap. Deposition* **2004**, *10*, 215.
(44) Kukli, K.; Kemell, M.; Puukilainen, E.; Aarik, J.; Aidla, A.; Sajavaara, T.; Laitinen, M.; Tallarida, M.; Sundqvist, J.; Ritala, M.; Leskelä, M. *J. Electrochem. Soc.* **2011**, *158*, D158.
(45) Kim, W.-H.; Park, S.-J.; Kim, D. Y.; Kim, H. *J. Korean Phys. Soc.* **2009**, *55*, 32.
(46) Aaltonen, T.; Ritala, M.; Tung, Y.-L.; Chi, Y.; Arstila, K.; Meinander, K.; Leskelä, M. *J. Mater. Res.* **2004**, *19*, 3353.